SpezialForschungsBereich F 32

Karl–Franzens Universität Graz
Technische Universität Graz
Medizinische Universität Graz

Receding horizon controller for the baroreceptor loop in a model for the cardiovascular system

Mark Mutsaers Mostafa Bachar Jerry Batzel
Franz Kappel Stefan Volkwein

SFB-Report No. 2007–001 June 2007

A–8010 GRAZ, HEINRICHSTRASSE 36, AUSTRIA

Supported by the
Austrian Science Fund (FWF)

SFB sponsors:

- **Austrian Science Fund** (FWF)
- **University of Graz**
- **Graz University of Technology**
- **Medical University of Graz**
- **Government of Styria**
- **City of Graz**

Receding horizon controller for the baroreceptor loop in a model for the cardiovascular system

Mark Mutsaers*; Mostafa Bachar, Jerry Batzel,
Franz Kappel and Stefan Volkwein †

Abstract

In this paper we discuss the design and implementation of a receding horizon control (RHC) which will be used to represent the control for the baroreceptor loop in the human cardiovascular system (CVS). This control will be applied to a model of the CVS developed by Kappel and Peer. In the earlier work, a linear quadratic control strategy (LQR) was implemented to represent this baroreflex control and it was designed to stabilize the system under an ergometric workload.

The RHC approach will be compared to the LQR implementation by estimation of the control parameters in the cost functional of the RHC utilizing experimental data used for validating the model in the earlier work.

1 Introduction

Over the past 50 years, many advances have been made in the area of modeling human cardiovascular physiology at the system level and in particular control mechanisms for such systems. This modeling has provided a great deal of information on qualitative and quantitative aspects of such systems. A primary long term goal of such research is to adapt such models to the clinical situation where predictions or diagnosis can be made that contribute to the treatment of the individual patient. A major problem in reaching that goal is that data is limited by the constraint of limiting invasive measurements. This poses a real challenge for model application requiring the development of new mathematical techniques for parameter estimation and new applications of current mathematical techniques such as RHC.

A number of examples of CVS models and modeling approaches can be found in [1] including the model developed by Kappel and Peer [2] which forms the basis for this current study. Most of the physiological features in that model

*Department of Electrical Engineering, Eindhoven University of Technology, The Netherlands.

†Institute for Mathematics and Scientific Computing, Karl-Franzens University Graz, Austria.

can be described via differential equations representing mass balance relations. However, the complex interacting elements in baroreflex control have not been completely described and the approach taken was to replace this control with a stabilizing control derived from optimal control theory. This model and the LQR approach will be described in detail in the next section (2).

Implementation of an LQR controller requires a linear or linearized model of the system. However, the Kappel and Peer model contains states defined by non-linear differential equations. By linearizing the model around an equilibrium state the LQR technique can be applied, but non-linear dynamics of the control would not be represented and the LQR is only a locally stabilizing control. For this reason, in this paper the LQR controller is replaced by the RHC which is a non-linear control approach introduced in Section 3.

After implementing this controller in a closed loop situation, control parameters are estimated to improve the control performance. These parameters are estimated by comparing simulation results with available clinical measurement data. This parameter estimation is discussed in Section 4 and simulation comparisons are given and compared to data in Section 5. Noise sensitivity is also discussed in this Section.

The receding horizon control implementation is compared with the LQR implementation in Section 6. In the last section some conclusions are drawn. Also some possible modifications are recommended for further research on this topic.

2 Description of the cardiovascular model

Before describing the Kappel and Peer model which will be the underlying model for this study, we discuss essential physiological features of the cardiovascular system. A block diagram for this system is given in Fig. 1. It can be seen in this figure that the heart is the central component of the system, linking together the pulmonary and systemic vascular circuits and providing the force to pump blood through these circuits. The heart is actually two synchronized pumps connected in series, containing the two ventricles, where blood for a single beat is collected. The pulmonary and systemic vascular loops are subdivided into arterial (high pressure) and venous (low pressure) vascular components and each of these contains many levels of branching vessels. In this model the multiple levels of vessels are lumped into four compartments: arterial systemic (as), venous systemic (vs), arterial pulmonary (ap) and venous pulmonary (vp) compartments. Each of these vascular compartments represents a blood volume, the vasculature has a certain compliance, and the state of each of these vascular compartments is characterized by the blood pressure of the compartment. For example P_{as} denotes arterial systemic blood pressure.

The flows in each circuit, generated by the cardiac output of the ventricles, is limited by the resistance to flows between vascular compartments. Given a set of parameters, it is possible to estimate the four states of the main vascular compartments (P_{as}, P_{vs}, P_{ap} and P_{vp}).

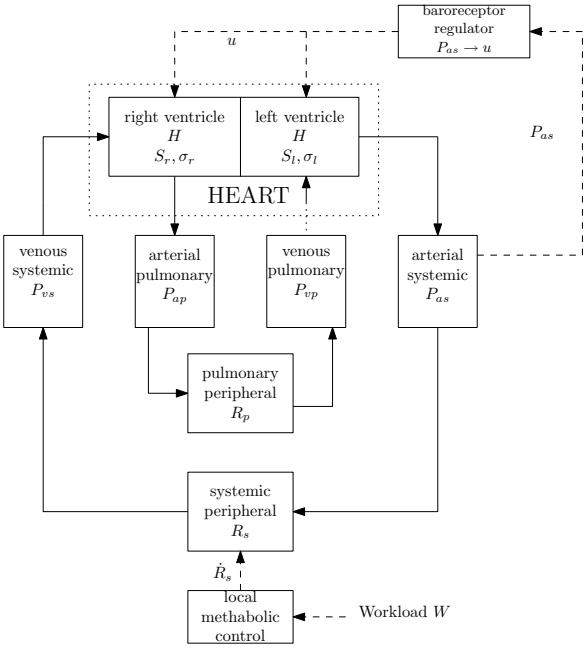

Figure 1: Block diagram of the cardiovascular model.

The resistance in the pulmonary loop (R_p) is fixed in the model, but the one in the systemic loop (R_s) depends on the workload of the person and his/her metabolic activity in particular. This workload influences the amount of oxygen that has to be supplied to the tissues. The variation in system resistance is determined by a local control mechanism which varies resistance in response to local metabolic activity. Because this control regulates the blood-flow by changing the resistance of the systemic loop, R_s is a state variable in the model.

The heart provides the blood pressure gradient to circulate blood through the tissues and lungs. Cardiac output (Q) is generated by the heart rate H and the strength of contraction of the ventricles. The contractilities of the the left and right ventricles are denoted by S_l and S_r, respectively. These contractilities are influenced by H with their relation described by a second order differential equation for each ventricle. This results in four first order differential equations, which are states in the model (S_l, σ_l, S_r and σ_r). The contractilities determine the output of one beat (stroke volume) which together with H determine cardiac output.

The heart rate is controlled by the baroreceptor loop. Sensors in the carotid artery and aortic arch measure arterial blood pressure P_{as} and send afferent nerve signals to the control center in the medulla which responds with efferent signals to modulate H. These nerve signals influence the frequency of the firing of cells that cause contraction of the ventricles. Because detailed understanding of this complex system is still under investigation, the modeling strategy was

implemented which replaced the baroreflex by a stabilizing LQR controller as described in [1]. This paper will consider the implementation of the RHC details of which can be found in [3, 4].

The Kappel and Peer model describing the cardiovascular system consists of ten states that can be described, at a any given time point as:

$$\underline{x} = [P_{as}, P_{vs}, P_{ap}, P_{vp}, S_l, \sigma_l, S_r, \sigma_r, R_s, H]^T \in \mathbb{R}^{10}.$$

The system's behavior is described by a set of (non-linear) differential equations:

$$\dot{\underline{x}}(t) = \mathcal{F}\left(\underline{x}(t), u(t)\right) \quad \text{with } t \in (t_b, t_e) \text{ and } \underline{x}(t_b) = \underline{x}_0. \tag{1}$$

Aortic systemic pressure and heart rate can easily be measured and are used as outputs (at a certain time moment):

$$\underline{y} = [P_{as}, H]^T \in \mathbb{R}^2.$$

The first of those two outputs (P_{as}) is used as input to the controller, which generates a control $u = \dot{H}$.

3 Receding horizon controller

In this section, another type of controller will be implemented to represent the action of the baroreceptor loop. As mentioned above, the LQR controller is designed for a linear (or linearized) system. However, the model for the cardiovascular system is non-linear, so a non-linear type of controller is desirable. The controller has to minimize the error between the current- and desired state, so an optimization problem needs to be introduced. We first describe the general optimization problem that needs to be solved in a receding horizon controller. Once the general problem is defined, the method can be applied to our model. With this optimization scheme it is possible to update the control output, as explained in Subsection *C*. The complete algorithm used in the controller is summarized in Subsection *D*. Once the controller is designed completely, it is possible to implement it in a closed loop situation, which is done in the last subsection.

3.1 General optimization problem

In the general case given in Equation (1) , we assume M input functions $\underline{u}$ where:

$$\underline{u} \in U = L^2\left(t_b, t_e : \mathbb{R}^M\right),$$

and t_b is the beginning and t_e is the end of each time interval used in the controller. Recall that the norm in U is given by:

$$||\underline{u}||_U = \sqrt{\int_{t_b}^{t_e} |\underline{u}(t)|^2 \, dt} \quad \text{for } \underline{u} \in U.$$

As the description of the model contains differential equations, the function space for the states X can not be of the same type as the function space for the inputs. However, the functions of the states $\underline{x}$ as well as the derivative with respect to time of these states $\dot{\underline{x}}$ should be in the same space. Given N state functions and the same time interval as used for the input functions $\underline{u}$, we have the following Sobolev space X where :

$$\underline{x} \in X = \left\{ \underline{x} \in L^2\left(t_b, t_e : \mathbb{R}^N\right) \mid \dot{\underline{x}} \in L^2\left(t_b, t_e : \mathbb{R}^N\right) \right\}.$$

The differential equations describing the system, and the cost function, are dependent on both the input functions $\underline{u}$ and the state functions $\underline{x}$. So, the product space Z, with functions $\underline{z} = (\underline{x}, \underline{u})$, is described by:

$$\underline{z} \in Z = X \times U.$$

Given these spaces, we describe the general cost function as follows:

$$\begin{aligned} J &: Z \to \mathbb{R} \\ (\underline{x}, \underline{u}) &\mapsto J(\underline{x}, \underline{u}). \end{aligned}$$

However, because of the constraints (1) give a relation between $\underline{x}$ and $\underline{u}$, valid solutions are only related to functions $\underline{u}$. This results in the following reduced cost:

$$\hat{J}(\underline{u}) = J(\underline{x}(\underline{u}), \underline{u}). \tag{2}$$

The optimization problem includes both a cost function and constraints and thus is referred to as a constrained optimization problem. These constraints are in general given by differential equations and their initial conditions: $\underline{x}(t_b) = \underline{x}_0$. In (1), the (non-linear) differential equations are given by $\mathcal{F} : \mathbb{R}^N \times \mathbb{R}^M \to \mathbb{R}^N$. The set of differential equations and their initial conditions can be rewritten with use of an operator $e(\underline{x}, \underline{u}) = e(\underline{z})$ as:

$$e = (e_1, e_2) : X \times U \longrightarrow L^2\left(t_b, t_e : \mathbb{R}^N\right) \times \mathbb{R}^N = Y \tag{3}$$

defined as:

$$(\underline{x}, \underline{u}) \longmapsto \begin{cases} e_1(\underline{x}, \underline{u}) = \dot{\underline{x}} - \mathcal{F}(\underline{x}, \underline{u}) & \in L^2(t_b, t_e : \mathbb{R}^N), \\ e_2(\underline{x}, \underline{u}) = \underline{x}(t_b) - \underline{x}_0 & \in \mathbb{R}^N. \end{cases}$$

Now the constrained optimization problem can be described as:

$$\min_{(\underline{x}, \underline{u})} J\left(\underline{x}, \underline{u}\right) \text{ subject to } e(\underline{x}, \underline{u}) = 0. \tag{4}$$

For this optimization problem the Lagrangian, which is utilized to derive optimality conditions, is given by:

$$\begin{aligned} L\left(\underline{x}, \underline{u}, \underline{\lambda}_1, \underline{\lambda}_2\right) = J\left(\underline{x}, \underline{u}\right) & \\ + \int_{t_b}^{t_e} \left(\dot{\underline{x}}(t) - \mathcal{F}\left(\underline{x}(t), \underline{u}(t)\right)\right)^T \underline{\lambda}_1(t) dt & \\ + \left(\underline{x}(t_b) - \underline{x}_0\right)^T \underline{\lambda}_2, & \end{aligned} \tag{5}$$

where $\underline{\lambda}_1 \in L^2(t_b, t_e : \mathbb{R}^N)$ and $\underline{\lambda}_2 \in \mathbb{R}^N$. If $(\underline{x}^*, \underline{u}^*) \in Z$ is an optimal solution to (4) then first-order necessary optimality conditions can be written as:

$$\nabla L\left(\underline{x}^*, \underline{u}^*, \underline{\lambda}_1^*, \underline{\lambda}_2^*\right) = 0, \tag{6}$$

where $\underline{\lambda}_1^*$ and $\underline{\lambda}_2^*$ are the dual or adjoint variables related to the constraints $e_1(\underline{x}^*, \underline{u}^*) = 0$ and $e_2(\underline{x}^*, \underline{u}^*) = 0$ respectively.

3.2 Optimization problem for the C.V. model

The model for the cardiovascular system contains of ten states ($\underline{x} : [t_b, t_e] \rightarrow \mathbb{R}^{10}$), described by a set of differential equations (1), and one input ($\underline{u} = u : [t_b, t_e] \rightarrow \mathbb{R}$).

In the model, two different equilibrium states (generally denoted with $\underline{x}^{eq}$) can be distinguished, which are the resting- ($\underline{x}^{rest}$) and the exercising phase ($\underline{x}^{exer}$). In the first part of the paper, the transition from the resting phase to the exercising phase is investigated, so $\underline{x}_0 = \underline{x}^{rest}$ and $\underline{x}^{eq} = \underline{x}^{exer}$. In Section V also the transition from exercise to rest is simulated.

Now the constraints (3) are known, the cost function has to be defined. In the baroreceptor loop, the arterial systemic pressure (P_{as}) is measured, so the difference between this value and the pressure in the desired equilibrium state is the first part of the cost function. The output of the controller is the change in heart rate, which should not be too large. That is why this controller output (u) is the second term in the cost. The last term of the cost function penalizes the final error in P_{as} at the end of the control interval ($t = t_e$). This should guarantee that the controller is stable.

So, the optimization problem can be described as:

$$\begin{aligned}
\min_{\underline{x},u} J\left(\underline{x}, u\right) = & \int_{t_b}^{t_e} \left(q_{as}^2 \left(P_{as}(t) - P_{as}^{eq}\right)^2 + \kappa_c^2 u(t)^2\right) dt \\
& + \frac{\alpha_c}{2} \left(P_{as}(t_e) - P_{as}^{eq}\right)^2 \\
\text{subject to} & \\
\dot{\underline{x}}(t) = & \mathcal{F}\left(\underline{x}(t), u(t)\right), \quad t \in (t_b, t_e), \\
\underline{x}(t_b) = & \underline{x}_0,
\end{aligned} \tag{7}$$

where q_{as}, κ_c and α_c are non-negative weighting factors that influence the behavior and the performance of the controller.

Now the first order optimality condition, described in (6), results in the gradients of the Lagrange function (5) with respect to the states $\underline{x}$ and to the controller output u. This first gradient gives the adjoint equations:

$$\begin{aligned}
& \dot{\underline{\lambda}}_1(t) + \mathcal{F}_{\underline{x}}(\underline{x}(t), u(t))^T \underline{\lambda}_1(t) - 2q_{as}^2 Q(\underline{x}(t) - \underline{x}^{eq}) = \underline{0} \\
& \underline{\lambda}_1(t_e) = -\alpha_c Q\left(\underline{x}(t_e) - \underline{x}^{eq}\right) \\
& \underline{\lambda}_2 = \underline{\lambda}_1(t_b),
\end{aligned} \tag{8}$$

with $t \in (t_b, t_e)$, $\mathcal{F}_{\underline{x}}(\underline{x}(t), u(t))$ is a matrix with the gradient of the set differential equations with respect to the states $\underline{x}$, $Q = \text{diag}(\underline{q}) \in \mathbb{R}^{10\times 10}$ with $\underline{q} = [1, 0, \ldots, 0]^T \in \mathbb{R}^{10}$.
The gradient with respect to the controller output u results in the optimality condition:

$$2\kappa_c^2 u(t) = \underline{\beta}^T \underline{\lambda}_1(t), \quad t \in (t_b, t_e), \tag{9}$$

where $\underline{\beta} = [0, \ldots, 0, 1]^T \in \mathbb{R}^{10}$. The derivation of those adjoint equations and the optimality condition are described in Section 3.4 and 3.5 of [5].

3.3 Updating controller output

By using the adjoint variable $\underline{\lambda}_1$ (see (8)) and the optimality condition (9), one can derive the gradient (with respect to the controller output u) of the reduced cost (2), which is described in Section 3.6 of [5]:

$$\nabla_u \hat{J}(u) = 2\kappa_c^2 u - \underline{\beta}^T \underline{\lambda}_1, \quad t \in [t_b, t_e]. \tag{10}$$

The total cost should be minimized by changing the controller output u for the time interval $t \in [t_b, t_e]$. To be sure that the controller output u does not exceed some bounds at any time moment in the interval, the gradient projection method [6] is applied. With this algorithm the nearest local minimum of the cost $\hat{J}(u)$ can be found. The update equation using this method for the new controller output $\hat{u}^{k+1}$ is described by:

$$\hat{u}^{k+1}(s) = P\left(\hat{u}^k - s\nabla_u \hat{J}(\hat{u}^k)\right) \quad \text{for } k \geq 0, \tag{11}$$

where P is the projection described by:

$$\begin{aligned} \hat{u}(t) = P(u(t)) = \begin{cases} a & : \quad u(t) \leq a, \\ b & : \quad u(t) \geq b, \\ u(t) & : \quad \text{otherwise}, \end{cases} \\ t \in (t_b, t_e), \end{aligned} \tag{12}$$

$\hat{u}^k$ is the previous (projected) controller output and $\hat{u}^{k+1}(s)$ is the updated controller output which depends on the variable $s \geq 0$. The value for s is chosen in such a way that the cost function decreases sufficiently and is found using backtracking with e.g. the Armijo rule. In the Armijo rule the norm of the reduced cost function ($||\nabla_u \hat{J}(u^k)||_U^2$) is used, which should go to zero if the solution is optimal. With the bounded versions of the controller's output, this norm is not always able to decrease to zero anymore. That is why this norm is replaced by the norm of the difference between the old and updated controller output ($||\hat{u}^k - \hat{u}^{k-1}||_U^2$), which results in the formula that is used during backtracking:

$$\hat{J}(\hat{u}^{k+1}(s)) \leq \hat{J}(\hat{u}^k) - sc||\hat{u}^k - \hat{u}^{k-1}||_U^2, \tag{13}$$

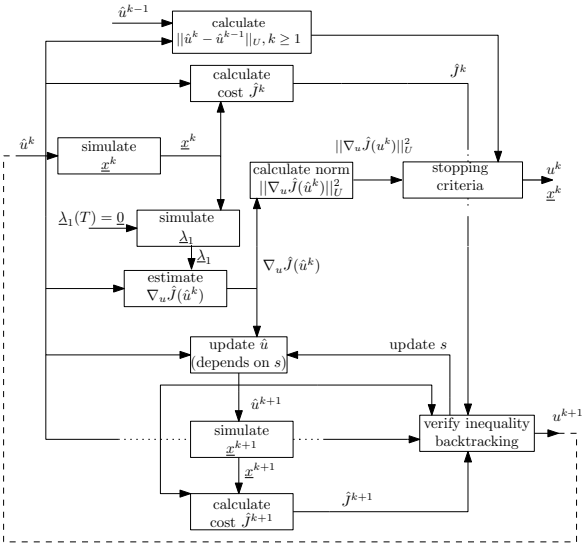

Figure 2: Algorithm used in the receding horizon controller.

where c is a small positive constant. If this condition doesn't hold, the value of s is divided by a factor two, and the values for the control output $\hat{u}^{k+1}$ in (11) are estimated again.

The values for the controller output for each time interval are updated till the relative- or absolute error in the norm of the reduced cost gradient ($||\nabla_u \hat{J}(\hat{u})||_U$) is small. The updating also stops when the controller output doesn't change that significant anymore (so if $||\hat{u}^k - \hat{u}^{k+1}||_U$ gets small) or if a maximal number of iterations has been reached.

3.4 Summary of complete algorithm

All previous steps done in this section of the paper are part of the complete algorithm in the receding horizon controller, which is depicted in Fig. 2.:

1. First of all, some starting value for the input u^0 and some initial conditions $\underline{x}_0$ have to be chosen. Those can be taken from literature or by doing some guesses based on simulations and measurements that are done earlier. The iterations are denoted by k, so $k = 0$ now.

2. For the input $\hat{u}^k$ the cardiovascular model for the state equations $\underline{x}^k$ can be solved for the complete time interval (using the initial conditions that are defined).

3. With the simulated values of the system's behavior, the cost function $\hat{J}^k$ can be estimated, which is used in the backtracking algorithm.

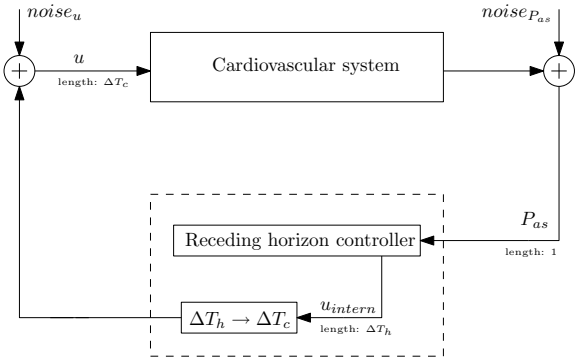

Figure 3: Closed loop situation with the different time intervals.

4. With the previous calculated state variables, the Lagrange multiplier function $\underline{\lambda}_1^k$ can be estimated. Using those values for the Lagrange multipliers, the gradient of the reduced cost ($\nabla_u \hat{J}(\hat{u}^k)$) and its norm ($||\nabla_u \hat{J}(\hat{u}^k)||_U^2$) can be computed.

5. If one of the stopping criteria holds, then a candidate for the optimal solution has been found! The values for $\hat{u}$ and $\underline{x}$ are stored in this situation, and the next time interval is simulated with the same algorithm. Now, the initial values for the states $\underline{x}^0$ are the last values from the previous simulation.

6. However, if the stopping criteria does not hold, the values for $\hat{u}$ are updated using (11) and projected using (12). The value of s has to confirm (13). If this condition doesn't hold, the value of s is divided by a factor two in the backtracking algorithm. When the condition holds, the new value for $\hat{u}^{k+1}$ is used as initial condition, so $k = k + 1$, and the algorithm starts at item 2) again!

3.5 Closed loop implementation

Now the functionality of the receding horizon controller is known, it can be implemented in a closed loop situation, which is depicted in Fig. 3. The output of the cardiovascular system is the arterial systemic pressure, which is fed back to the receding horizon controller at a certain time moment $t = t_b$. The receding horizon controller starts to predict the behavior of the system for the time horizon from $t = t_b$ till $t = t_e$, which is named ΔT_h from now on. The interval of the controller output itself does not have to be the same as this horizon of course. The prediction horizon is therefore defined as $\Delta T_h = K_\Delta \Delta T_c$, where ΔT_c is the length of the interval the controller gives output. We must also have $K_\Delta \geq 1$ because $\Delta T_c \leq \Delta T_h$. After this control interval the new value for P_{as} at time $t = t_b + \Delta T_c$ is read by the receding horizon controller and the procedure starts over again.

The controller has to behave stable when noise is added to the output in the closed loop situation. Also an addition of noise on the input of the system should not result in unstable behavior of the controller. Those noise additions are investigated in the section with simulation results.

There are five possible parameters that can influence the performance and behavior of the controller: the parameters in the cost function (q_{as}, κ_c and α_c), the time interval of the prediction horizon in the controller (ΔT_h) and the ratio of this interval that is used as output of the controller (K_Δ). The closed loop system should match reality, so there parameters are determined in the next section of this paper.

4 Parameter estimation

Because real measurement data for the arterial systemic pressure and the heart rate during a transition from the resting- to the exercise phase are available, an estimation for the parameters in the receding horizon controller can be performed. The estimation is done using an optimization problem, which is described by:

$$\begin{aligned} \min_{\underline{p}} R(\underline{p}) = & \int_0^T |H^{sim}(t,\underline{p}) - H^{meas}(t)| \\ & + |P_{as}^{sim}(t,\underline{p}) - P_{as}^{meas}(t)| \; dt, \\ \text{subject to } & \underline{p} \geq \underline{0} \text{ and } K_\Delta \geq 1, \end{aligned} \tag{14}$$

where $\underline{p}$ is the set of parameters which are estimated and $H^{sim}(t,\underline{p})$ and $P_{as}^{sim}(t,\underline{p})$ are the values for the heart rate and arterial systemic pressure estimated using the closed loop system with the receding horizon controller. $H^{meas}(t)$ and $P_{as}^{meas}(t)$ are the measured data values for those two states. (14) is a bi-level optimization problem since (H^{sim}, P_{as}^{sim}) are computed by solving an optimization problem for fixed $\underline{p}$.

The identification of the parameters is done in multiple steps, because several problems occurred: the appearance of local minima for the parameter K_Δ and the approximation of the numerical gradient for the time interval ΔT_c.

After estimating values for those two parameters, the control parameters are estimated using the Optimization Toolbox of Matlab. This results in the following set of optimal parameters:

$$\begin{aligned} \underline{p}_1^* &= [\Delta T_c^*, K_\Delta^*, q_{as}^*, \kappa_c^*, \alpha_c^*]_1 \\ &= [0.4, 2, 0.0241, 0.0185, 0.7099]\,. \end{aligned}$$

With this set of parameters, the cost has been decreased from a value of $R(\underline{p}_1^0) = 56.9638$ with an initial set of parameters ($\underline{p}_1^0 = [0.4, 2, 0.4, 0.3181, 0.8]$) to a value of $R(\underline{p}_1^*) = 53.8218$ with the estimated ones. The simulation of the system with

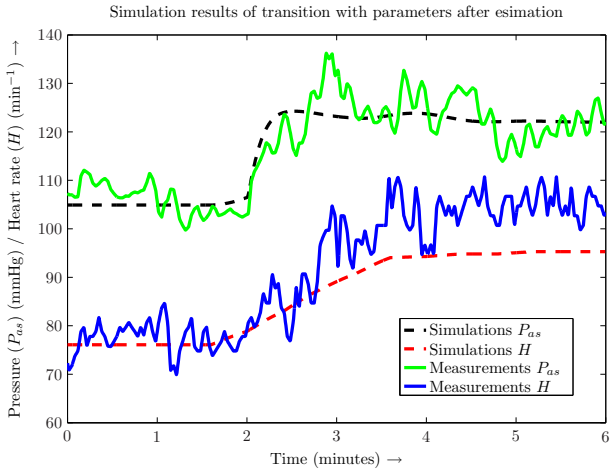

(a) Simulations results and measurement data of H and P_{as}.

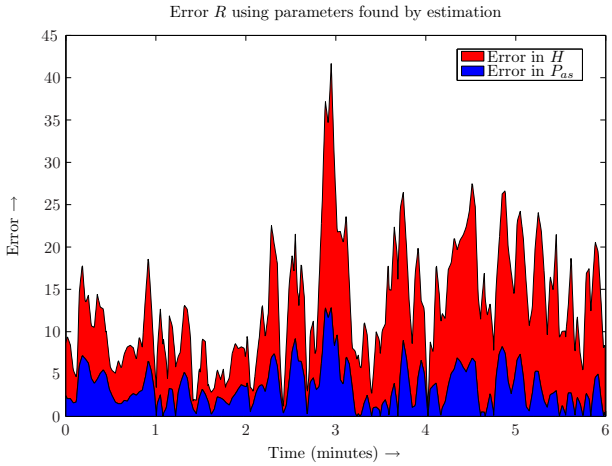

(b) The absolute errors between simulations and measurements.

Figure 4: Results of parameter estimation for the control parameters: $\underline{p}_1^* = [\Delta T_c, K_\Delta, q_{as}, \kappa_c, \alpha_c] = [0.4, 2, 0.0241, 0.0185, 0.7099]$.

State:	Resting phase:	Exercising phase:
P_{as}	105 mmHg	122 mmHg
H	80 min^{-1}	105 min^{-1}

Table 1: Values of the states P_{as} and H in the equilibrium states.

this set of parameters is depicted in Fig. 4(a). and in Fig. 4(b). the absolute error between the measurements and simulation data is shown.

One can see that there is still an error in the value of the heart rate (H) after the transition from resting- to exercising phase. This can be solved by estimating in addition some parameter values of the model (c_l and c_r) [1], that were estimated when the LQR-controller was implemented. This change in model parameters can influence the optimal parameters of the controller, so they also need to be estimated again. The parameter set found by the optimizer is:

$$\begin{aligned}\underline{p}_2^* &= [\Delta T_c^*, K_\Delta^*, q_{as}^*, \kappa_c^*, \alpha_c^*, c_l^*, c_r^*]_2 \\ &= [0.4, 2, 0.0881, 0.03741, 0.12, 0.01062, 0.08543]\,.\end{aligned}$$

Those parameters are used in simulations which resulted Fig. 5., where can be shown that the error in the value for the heart rate has disappeared. The value of the cost $R(\underline{p}_2^*)$ has been reduced to 42.1777.

5 Simulation results

In the previous section of this paper a set of parameters is estimated that are used in the next simulations. In the simulations done in this section of the paper also an initial error in the value of P_{as} of 15 mmHg and the transition from exercise phase to resting phase are simulated. In Fig. 6(a). and Fig. 6(b). the output of the controller u, which is the input of the system, and the outputs of the system H and P_{as} are depicted. The values for the equilibrium states H and P_{as} defined in the receding horizon controller are given in Table 1, and can also be distinguished in the plot of the simulation results. The controller compensates for the initial error and drives the system to the state for the resting phase. Also the transitions between the difference states are controlled fast with not that large controller outputs.

Noise sensitivity

As depicted in Fig. 3. noise can be added to two signals in the system: the system output P_{as}, which is fed back to the controller, and the output of this controller u. In the real system, this are the signals that travel from the baroreceptors to the medulla and those that go back to the heart. Because those signals have to pass the nerve system, which also processes a lot of other signals at the same time, it is reasonable to assume that it is possible that some noise is added to those signals.

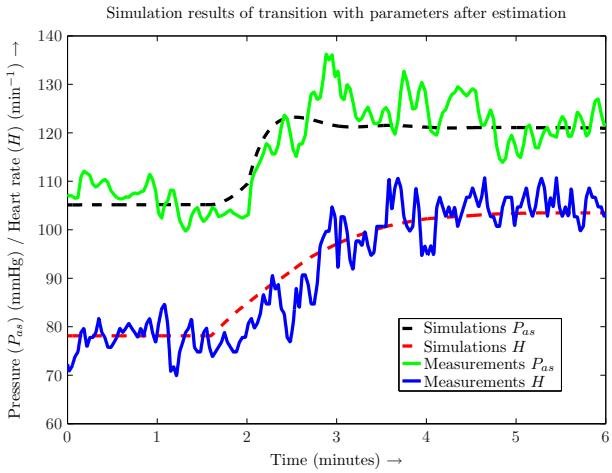

(a) Simulations results and measurement data of H and P_{as}.

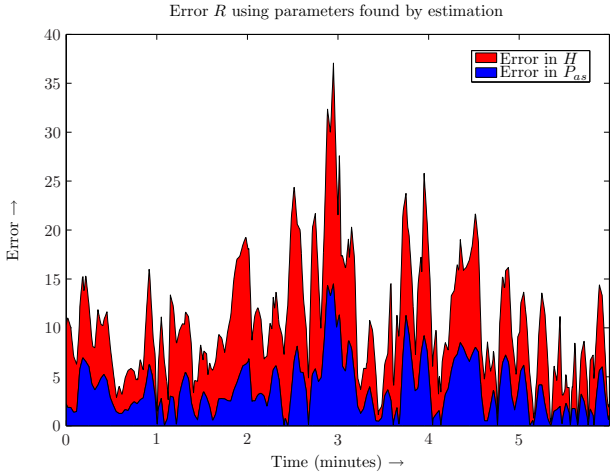

(b) The absolute errors between simulations and measurements.

Figure 5: Results of parameter estimation for the parameter-set: $\underline{p}_2^* = [\Delta T_c, K_\Delta, q_{as}, \kappa_c, \alpha_c, c_l, c_r] = [0.4, 2, 0.0881, 0.03741, 0.12, 0.01062, 0.08543]$.

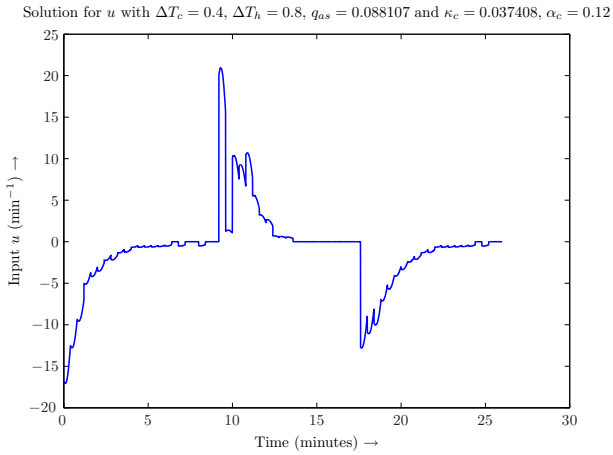

(a) Input u from the controller

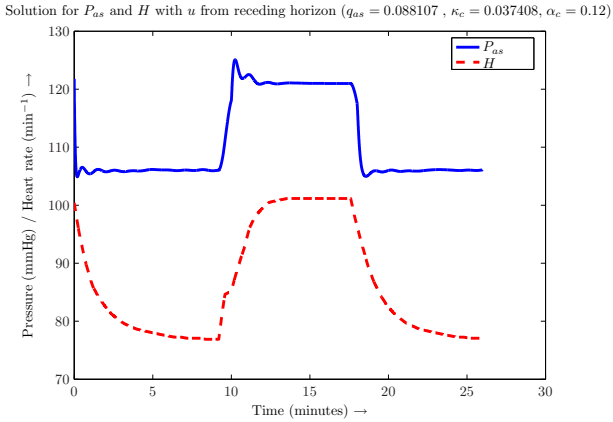

(b) Controlled states P_{as} and H

Figure 6: Results of closed loop system without addition of noise.

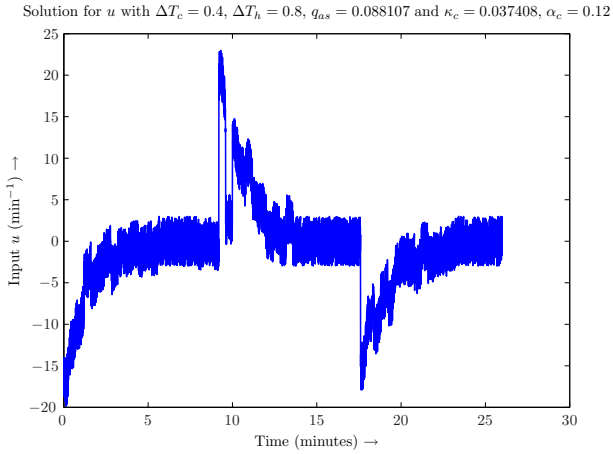

(a) Input u from the controller

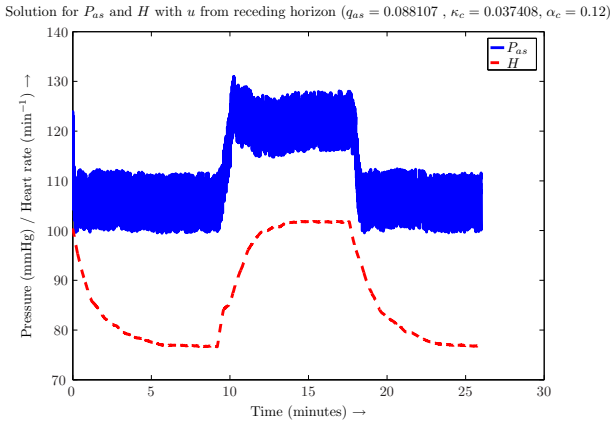

(b) Controlled states P_{as} and H

Figure 7: Results of closed loop system with addition of noise to both the system in- and output ($u \pm 3$ min^{-1} & $P_{as} \pm 6$ mmHg).

Simulations with additions of white noise with a certain amplitude (± 3 min^{-1} for the change in the heart rate and ± 6 mmHg for the noise in the arterial systemic pressure) have resulted in a system that still behaves stable. This is depicted in Fig. 7., where it can be seen that the closed loop system is still stable.

6 Comparison with LQR controller

A detailed comparison with the results obtained with the LQR controller is not possible at this stage of the investigations. The reason is that a careful parameter identification procedure, which involves all parameters of the receding horizon controller and the cardiovascular model (as done before for the system when using the LQR controller [1]), has to be done. This is clear from the results presented at the end of Section IV.

A preliminary comparison of the two control strategies considering a different aspect of the system is done. The feedback control u is perturbed by normally distributed noise and the model outputs $P_{as}(t)$ and $H(t)$ are sampled with the same frequency as the one used to perturb u (sampling frequency = 0.5 Hz). Fig. 8(a). and 8(b). are presenting the eigenvector pseudospectra of H respectively P_{as} for the data as well as for the model outputs obtained with the LQR controller and the receding horizon controller. The pseudospectra are given in terms of a normalized frequency, where the value 1 corresponds to the Nyquist frequency, which equals to half the sampling frequency, i.e., to 0.25 Hz. The pseudospectra were obtained by the function **spectrum.eigenvector** of Matlab's Signal Processing toolbox (compare also [7]). At this step of the work it can be said that the receding horizon control certainly provides a feasible alternative to the linear quadratic control approach.

7 Conclusions and Future Work

Receding horizon control has been successfully used for control of systems with non-linearities, with uncertainties and with constraints for control and state variables in technical applications. Therefore it was quite natural to use receding horizon control also in the context of the cardiovascular system for modeling the functioning of the baroreceptor loop and other control loops. In this paper we did a first step into this direction by considering a very basic model for the reaction of the cardiovascular system to an ergometric workload. We could show that receding horizon control offers a feasible alternative to the LQR-approach which has been used previously. On the basis of the work presented in this paper we plan to consider the more complex models used for orthostatic stress situations where several interacting control loops play an important role (see for instance [9]). We also plan to utilize this control strategy in cases where state constraints are important, as for instance in models for the reaction of the cardiovascular system to hemorrhage (see [8]).

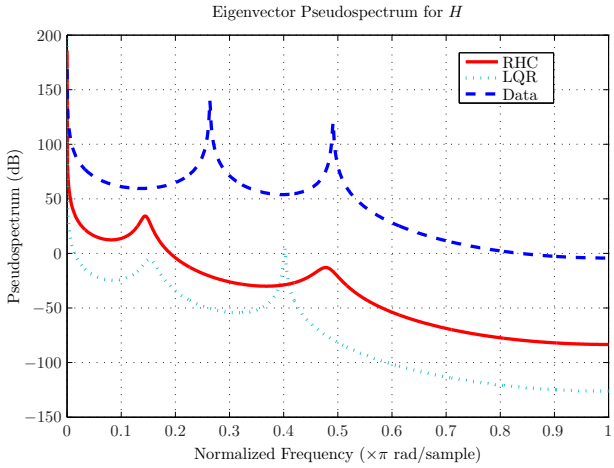

(a) Eigenvector pseudospectra for H.

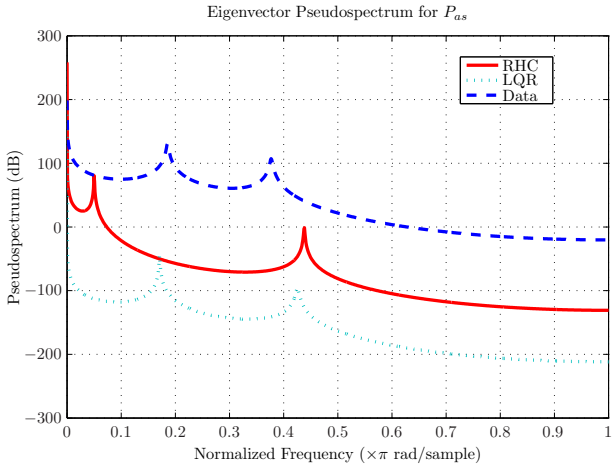

(b) Eigenvector pseudospectra for P_{as}.

Figure 8: Comparisons made between the LQR and the receding horizon controller.

References

[1] J.J. Batzel, F. Kappel, D. Schneditz and H. Tran, *Cardiovascular & Respiratory Systems: Modeling, Analysis & Control*, SIAM, Graz/Raleigh, 2005.

[2] F. Kappel, and R. Peer, *A mathematical model for fundamental regulation processes in the cardiovascular system*, J. Math. Biol., 31 (1993), pp. 611-631.

[3] F. Allgöwer, T. Badgwell, J. Qin, J. Rawlings and S. Wright, *Nonlinear predictive control and moving horizon estimation - An introductory overview*, in Advances in Control, P. Frank, ec., Springer, London, 1999, pp. 391-449

[4] C.E. Garcia, D.M. Prett and M. Morari, *Model predictive control: Theory and practice - a survey*, Automatica, 25 (1989), pp. 335-348.

[5] M.E.C. Mutsaers, *Receding horizon control techniques applied to the cardiovascular system*, Technical Report IMA23-07, http://www.uni-graz.at/imawww/reports/index.html, Institute for Mathematics and Scientific Computing, Graz, 2007.

[6] C.T. Kelley, *Iterative Methods for Optimization*, SIAM, Philadelphia, 1999.

[7] S.L. Marple, *Digital Spectral Analysis*, Prentice-Hall, Englewood Cliffs, NJ, 1987.

[8] J.J. Batzel, M. Fink and F. Kappel, *Modeling the human cardiovascular-respiratory control response to blood volume loss due to hemorrhage*, Lecture Notes in Control and Information Sciences, Vol. 341, pp. 145-152, Springer-Verlag, Berlin, 2006.

[9] F. Kappel, M. Fink and J.J. Batzel, *Aspects of control of the cardiovascular-respiratory system during orthostatic stress induced by lower body negative pressure*, Math. Biosciences, pp. 273-308, 2007.

E-Mails: M.E.C.Mutsaers@student.tue.nl;
mostafa.bachar,jerry.batzel,franz.kappel,stefan.volkwein@uni-graz.at.

Acknowledgements: This research was partially funded by FWF (Austria) project P18778-N13. The author S.V. also gratefully acknowledge support by the SFB Research Center "Mathematical Optimization and Applications in Biomedical Sciences" (SFB F32).